4 ACCIDENT PHENOMENA

4.1 INTRODUCTION

Equally as important as the identification hazards (Chapter 3) are the mechanisms with which these hazards occur and propagate. In the following subsections the mechanisms and consequences associated with the evolution of a flammable gas cloud, ignition, combustion and the resultant thermal radiation and generation of pressure waves are discussed. Regarding the evolution of a flammable gas cloud, the transport mechanism of jet releases, three-dimensional diffusion (Navier-Stokes) and general considerations regarding the overall dispersion of a gas cloud are considered. With respect to combustion, the general types of flames (laminar and turbulent) and combustion modes (deflagration, detonation and DDT) and their consequences (thermal radiation and blast waves) are reviewed.

4.2 EVOLUTION OF A FLAMMABLE GAS CLOUD

The release and distribution of a flammable gas depend on its thermodynamic state during storage and pressurized gases will form a free jet or be flash released in case of containment failure. The parameters of concern associated with the release of a flammable substance include (Verfondern & Nishihara, 2005):

- expansion of a flammable vapour cloud,
- height a flammable cloud could reach,
- time required for dilution to below LFL, and
- total quantity of combustible fuel in the cloud.

The spreading and dispersion behaviour of a gas depends significantly on the density difference between the gas and the surrounding air as well as ambient conditions such as wind and moisture content. Gases with low buoyancy or are heavier-than-air disperse slowly into the surrounding air and therefore tend to accumulate in the low-lying areas close to the point of release. These gases rely on the ambient airflow for dispersion (in the downstream direction of the wind) and only a small portion of the cloud may be within the flammability limits. If the conditions (atmospheric and gas density) are such that the leakage rate is larger than the removal rate (dispersion and *etcetera*), a vapour blanket can accumulate on the ground until a certain size is reached under steady-state conditions (Verfondern & Nishihara, 2005).

If a cold gas is released or if the gas cools upon release (from a highly pressurized vessel), it causes the moisture in the air to condense and make the cloud visible. The presence of droplets, either liquefied gas or ambient moisture, can result in condensation and vaporization processes that remove or add heat to the gas cloud. The lower the ambient moisture content, the larger the life span of vapour clouds that are heavier-than-air (or low buoyancy) and therefore increase the total quantity of fuel in the cloud as well as improving the probability of ignition (Verfondem & Nishihara, 2005).

The downwind distance that a flammable cloud could travel is smaller for facilities that have obstructions or congestions than for open land due to the increased generation of turbulence, which consequently results in faster dilution of the cloud. However, these barriers are less effective at higher wind speeds or very large releases and may result in a significant accumulation of the flammable substance at specific locations (Verfondern & Nishihara, 2005).

4.2.1 JET RELEASES

The release of hydrogen through a hole or aperture from a pressurized container occurs as a "jet" release due to the positive pressure difference between the container and its environment and may be sonic (choked) or subsonic depending on the upstream pressure. The flow resulting from a subsonic release is essentially an expanded jet and has a hydrogen concentration profile inversely proportional to the distance to the nozzle (aperture) along the axis of the jet. It is suggested that the axial concentration (by volume) decay of variable-density subsonic jets occurs according to a Gaussian function centred on the jet axis, given by the following equation (BRHS, 2007; Chen & Rodi, 1980 as cited in BRHS, 2007):

$$\frac{C(x)}{C_j} = K\frac{d_j}{x-x_0}\left(\frac{\rho_a}{\rho_g}\right)^{1/2} \qquad \textbf{Equation 4-1}$$

Where:

$C(x)$	Concentration by volume at position x along jet axis [mol/m^3]
C_j	Concentration by volume at the outlet nozzle [mol/m^3]
d_j	Discharge diameter [m]

ρ_a	Density of the ambient air [kg/m^3]
ρ_g	Density of the gas at ambient conditions [kg/m^3]
x	Distance from the nozzle along the jet axis [m]
x_0	*Virtual absicca of the hyperbolic decrease [m]*
K	Constant (equal to 5) [-]

With respect to hydrogen, subsonic releases occur while the upstream pressure is below 1.9 times that of the downstream pressure, whereas sonic releases occur beyond that point. Furthermore, while the flow rate of a sonic release depends only on the upstream pressure, the flow rate of a subsonic release depends on the pressure difference between the upstream and downstream pressures. Considering a pressurized gaseous hydrogen system open to atmospheric conditions, the release of hydrogen from an aperture or orifice occurs under sonic conditions while the containment pressure remain in excess of 1.89 bar (BRHS, 2007).

During sonic releases of hydrogen, the gas velocity at the exit of the nozzle is equal to the sonic velocity of the gas, which is 1294 m/s in pure hydrogen at NTP and 975 m/s in a stoichiometric hydrogen-air mixture at NTP. The mass flow rate exiting the pressurized containment can therefore be estimated from the following equation (BRHS, 2007):

$$\dot{m} = \rho A c \qquad \textbf{Equation 4-2}$$

Where:

$\dot{m}$	Mass flow rate [kg/s]
ρ	Density of hydrogen at the exit of the nozzle [kg/m^3]
A	Cross sectional area of the nozzle opening [m^2]
c	Sonic (sound) velocity of the gas [m/s]

However, Equation 4-2 is only an approximation and the shape of the aperture, friction and the length of the conduit between the reservoir and the release point influence the actual mass flow rate. Additionally, (de)pressurization affects temperature while temperature affects sonic velocity, whereas both and temperature and pressure affect exit gas density, resulting in a sonic mass flow rate that varies as the upstream pressure drops (BRHS, 2007).

A choked jet essentially consists of two regions, namely an under-expanded and expanded region. In the under-expanded region the flow rate becomes supersonic and forms a cone-like structure (known as a Mach cone), whereas the flow in the expanded region behaves similar to that of an expanded subsonic jet (BRHS, 2007).

The axial concentration decay of sonic releases differs to that of subsonic releases (Equation 4-1) only in that the discharge diameter is replaced by an effective diameter, which is representative of the jet diameter at the start of the subsonic region (after the Mach cone) and may be estimated through the following equations (BRHS, 2007):

$$\frac{C(x)}{C_j} = K\frac{d_{eff}}{x-x_0}\left(\frac{\rho_\alpha}{\rho_g}\right)^{1/2} \qquad \textbf{Equation 4-3}$$

With:

$$d_{eff} = \left(\frac{\rho_j u_j}{\rho_g u_{eff}}\right)^{1/2} d_j \qquad \textbf{Equation 4-4}$$

$$u_{eff} = u_j + \frac{p_j - p_\alpha}{\rho_j u_j} \qquad \textbf{Equation 4-5}$$

Where:

d_{eff}	Effective jet diameter [m]
u_j	Velocity of the jet at the outlet [m/s]
u_{eff}	Effective velocity of the gas [m/s]
p_j	Pressure at the jet outlet [kPa]
p_α	Ambient Pressure [kPa]

This approach is that proposed by Birch *et al.* (1987) and calculates the effective diameter and corresponding effective velocity by applying the conservation of mass and momentum between the outlet and a position beyond the Mach cone where the pressure first becomes equal to that of the ambient pressure and assumes no entrainment of ambient air (BRHS, 2007). The value of the constant K differs significantly according to the specific gas undergoing depressurization as well as the containment conditions (pressure) and aperture dimensions. The following figure

(Figure 4-1) illustrates the distances to hydrogen molar concentrations of 2.0%, 4.0%, 6.0%, and 8.0% from a 207.85 bar tank for various leak diameters by using the Sandia/Birch approach (BRHS, 2007; Houf & Shefer, 2006 as cited in BRHS, 2007).

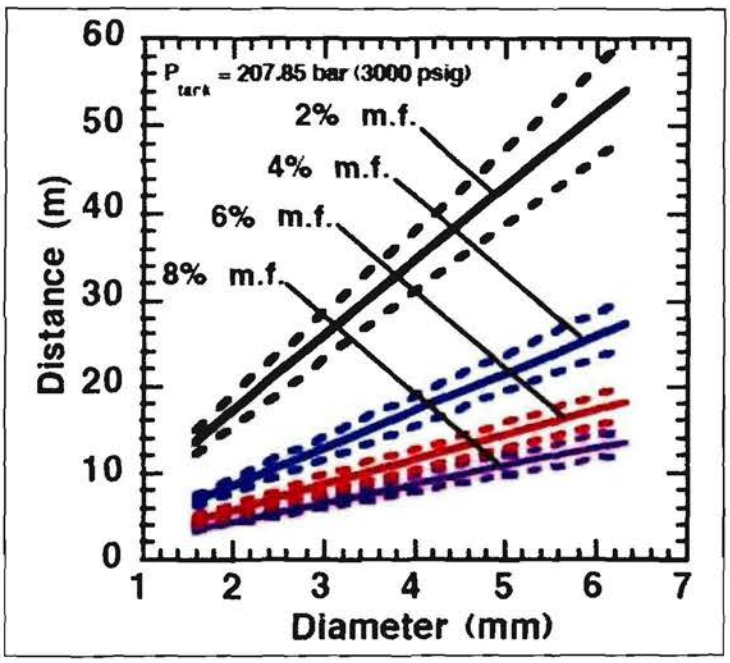

Figure 4-1: Distance vs. aperture diameter for various concentrations (Houf & Shefer, 2006 as found in BRHS, 2007)

The dashed lines indicate the upper and lower bounds resulting from a ± 10 % uncertainty in the value of the constant K (BRHS, 2007). From this figure, it is evident that a (flammable) gas could travel a very significant distance by being jet released from a pressurized container and necessitate thorough precautionary measures be taken to avoid such a depressurization accident.

4.2.2 DIFFUSION

Diffusion ($\vec{J_i}$) is the transport of molecules due to a concentration-, temperature- or pressure gradient and are respectively known as ordinary diffusion ($\vec{J_i^d}$), thermal diffusion ($\vec{J_i^T}$) and pressure diffusion ($\vec{J_i^p}$). The general equations describing the overall and respective multi-group diffusion rates are (Warnatz *et al*, 2006):

$$\vec{J_i} = \vec{J_i^d} + \vec{J_i^T} + \vec{J_i^P}$$ **Equation 4-6**

$$\vec{J_i^d} = \rho_i \vec{V_i} = \frac{\rho M_i}{M^2} \sum_{(i\,not=1)} D_{ij}^{mult} M_j \, grad\, x_j$$ **Equation 4-7**

$$\vec{J_i^T} = -D_i^T \, grad\,(\ln T)$$ **Equation 4-8**

$$\vec{J_i^P} = \frac{\rho M_i}{M^2} \sum_{(i\,not=1)} D_{ij}^{mult} M_j \left(x_j - w_j\right) grad\,(\ln p)$$ **Equation 4-9**

With:

$\vec{J}$	Mass flux [kg/s.m^2]
M	Molecular weight [kg/mol]
D_{ij}	Diffusion coefficient [cm^2/s]
x	Mole fraction [-]
w	Mass fraction [-]

Diffusion plays a relatively minor role in the overall dispersion of a gas cloud and should not be confused with any other transport phenomena (Warnatz *et al*, 2006). However, molecular diffusion is responsible for the transport of hydrogen through metals, which causes hydrogen embrittlement, and may lead to tritium contamination of the chemical process, and possibly hydrogen ingress into the nuclear cycle.

4.2.3 DISPERSION OF GAS CLOUDS

Dispersion of gas clouds is a somewhat complex issue and is the subject of many investigations, especially the numeric solution of dispersion models enjoy a great deal of attention. Understanding hydrogen behaviour during and after its unintended release from a pressurized containment is an important phase in developing sufficient mitigation measures such as safety distances and protective barriers (Cheng *et al.*, 2005). If public acceptance is to be achieved for the so-called hydrogen economy, accurate models need to be in place to predict the dispersion behaviour of hydrogen gas following its inadvertent release from a pressurized containment. To this extent, several studies focus on numerically solving the dispersion of hydrogen with regard to the flammable concentrations of hydrogen gas in air under various ambient conditions.

Cheng *et al.* (2005) investigated the discrepancy between applying the Ideal Gas Law and Real Gas Law (three-dimensional compressible Navier-Stokes Equations

incorporated with the Able-Noble Equation of State) for sonic releases of hydrogen into ambient conditions. Significant differences were obtained regarding the release rate as well as the corresponding vapour cloud dimensions as are shown in the following figure (Figure 4-2) and table (Table 4-1).

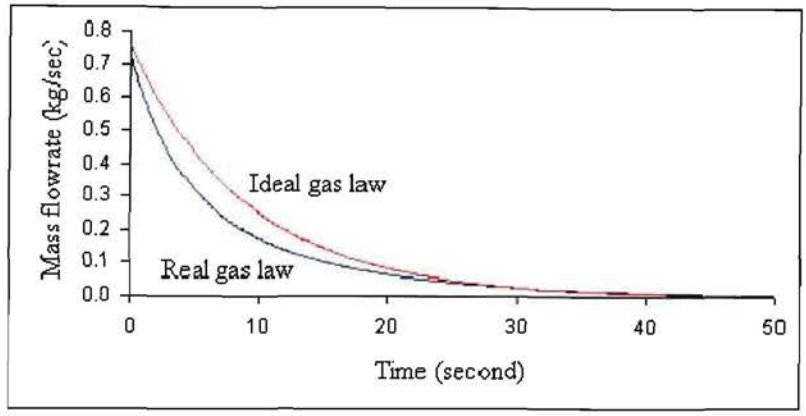

Figure 4-2: Comparison of the mass flow rate following a sonic release of hydrogen according to the Ideal gas law and Real gas law Cheng *et al.* (2005)

From this figure, it is clear that the Ideal Gas Law overestimates the hydrogen mass release rate during the initial 25 seconds, after which it is comparable to that of the Real Gas Law. The authors found that the Ideal Gas Law overestimates the total amount of hydrogen released during the initial 25-second period by as much as 35 % (Cheng *et al.*, 2005) and conclude that Real Gas Law(s) should rather be applied. Table 4-1 shows the dimensions of the hydrogen cloud related to the LFL of hydrogen at various times after initiation of the release. As expected, the Ideal Gas Law yet again overestimates.

Table 4-1: Hydrogen cloud extents according to numerical solutions of the Ideal gas law and Real gas law at 3, 5, 20 and 40 seconds after release (Cheng *et al.*, 2005)

Time	Concentration	Ideal gas law		Real gas law	
		Horizontal	Vertical	Horizontal	Vertical
3 seconds	200% of LFL	3.11 m	1.37 m	2.82 m	1.35 m
	LFL	5.04 m	2.60 m	4.65 m	2.48 m
	50% of LFL	6.84 m	5.12 m	6.41 m	4.85 m
5 seconds	200% of LFL	2.95 m	1.37 m	2.82 m	1.25 m
	LFL	5.11 m	2.61 m	3.80 m	2.35 m
	50% of LFL	7.82 m	5.40 m	7.11 m	5.11 m
20 seconds	200% of LFL	3.35 m	0.79 m	3.34 m	0.78 m
	LFL	6.45 m	2.07 m	6.40 m	2.02 m
	50% of LFL	11.85 m	5.05 m	11.80 m	5.03 m
40 seconds	200% of LFL	3.21 m	0.78 m	3.20 m	0.78 m
	LFL	6.01 m	2.12 m	6.02 m	2.12 m
	50% of LFL	11.77 m	6.00 m	11.74 m	6.10 m

Moreover, the authors found that the sonic release of hydrogen from a 205 L container at 400 bar, through a 6 mm pressure relief device (PRD), has the following hydrogen volumetric concentration distributions at 3 and 5 seconds after initiation of the leakage according to the Ideal Gas Law and Real Gas Law (Figure 4-3).

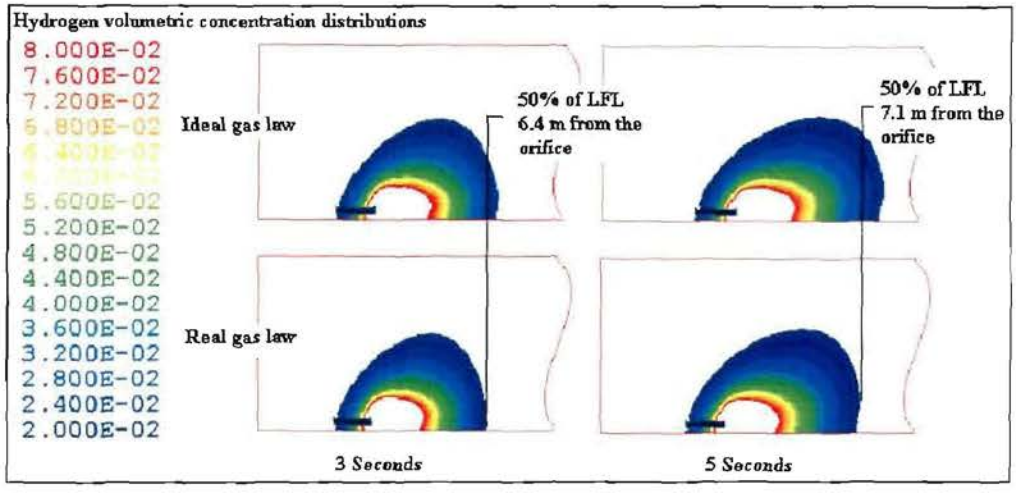

Figure 4-3: Hydrogen concentrations at 3 and 5 seconds after leak according to numerical solutions of the Ideal gas law and Real gas law (Cheng *et al.*, 2005)

The investigation of Cheng *et al.* (2005) considered a horizontal leak at 0.5 m elevation above-ground, a wind velocity of 0.5 m/s in the direction of the leak, and ambient temperature of 20 ^{0}C. Considering Figure 4-3, at 3 seconds after the onset of release, the horizontal extent of the hydrogen-air cloud at 2 % hydrogen concentration according to the Ideal Gas and Real Gas laws are respectively 6.41 m and 6.84 m. After 5 seconds, the Ideal Gas Law overestimates the different hydrogen concentrations by more than 10 %, which corresponds to approximately 20 to 30 % increased hydrogen cloud volumes and is due to the Ideal Gas Law overestimating the release rate by about 25 % after 5 seconds (Cheng *et al.*, 2005).

Granovskiy *et al.* (2004) investigated the dispersion behaviour of a hydrogen gas cloud with volume of 799.2 m^3 and showed the effects of wind speed and obstructions on the hydrogen mass concentration distributions (Figure 4-4).

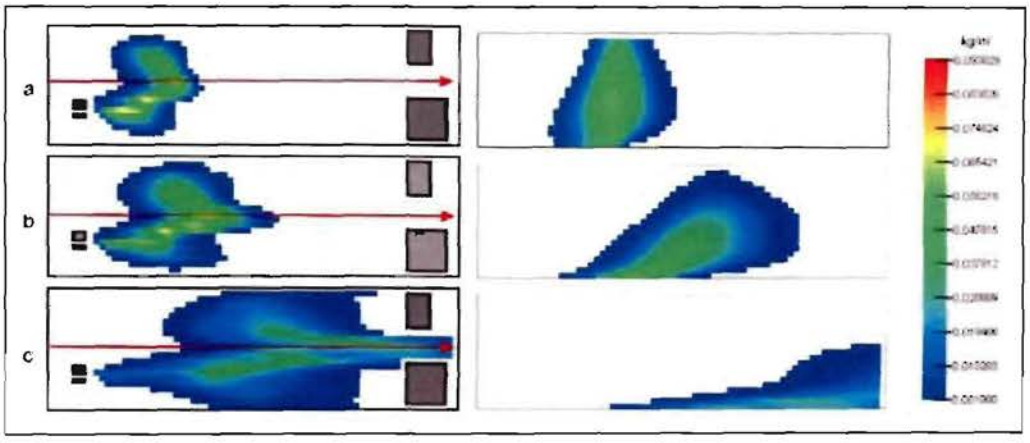

Figure 4-4: Hydrogen concentration distribution in 5 seconds after release with a wind speed of a) 1 m/s b) 3 m/s and c) 10 m/s (Granovskiy *et al.*, 2004)

It is clear from Figure 4-4 that hydrogen's high buoyancy is essential only at low wind speeds and that the presence of obstructions in close vicinity to the point of release is very dangerous. When the wind speed is greater than hydrogen's buoyancy (≈ 1.2 m/s) it behaves as a neutral gas and conforms to the directional movement of the ambient air, as well as accumulating near-ground due to the no-slip boundary condition. The presence of obstructions increases the accumulation of hydrogen before the obstructions and accelerates dispersion between them. Therefore, the lifetime of a flammable gas cloud between the point of release and the obstructions is extended, while the increased concentrations also enhance the associated hazards related to thermal radiation and blast waves when the gas cloud is ignited. Moreover, due to the gas cloud's tendency to layer near-ground when exposed to a sufficiently strong ambient wind velocity, the horizontal distance a flammable gas cloud could travel (possibly to an ignition source) is significantly increased.

4.2.4 REAL GAS CLOUDS

A real gas cloud differs significantly from the ideal gas cloud and involves aspects such as non-premixed states, inhomogeneous concentration distribution and air entrainment at the boundaries. These (and other) deviations from the ideal situation are able to either increase or decrease the pressure build-up in the gas cloud. Aspects such as non-stoichiometry and ignition at the cloud edge decrease the pressure build-up, whereas the real gas cloud (flat, long-stretched) may experience multi-point ignition, more turbulence generating terrain roughness and obstacles in its flow path, all of which enhance the pressure build-up. The most probable scenario in

a chemical plant is the release of a flammable gas from a high-pressure vessel resulting in a rising and expanding fireball if ignited (Verfondern & Nishihara, 2005).

The realistic shape of a heavy gas cloud is of pancake form and covers an area larger than the hemispherical cloud but contains the same explosive inventory. The propagation of a flame in such a cloud is (initially) spherical until it reaches the upper cloud boundary, after which it continues only in the horizontal direction. The pressure decreases immediately behind the flame front and the peak overpressures outside the cloud are slightly higher for flat clouds than spherical clouds, but the pulse duration of the blast wave is shorter (Geiger, 1980 as cited in Verfondern & Nishihara, 2005).

The following two figures (Figures 4-5 & 4-6) compare the deflagration and detonation of an ideal hemispherical cloud with that of a real, pancake shaped cloud. During a deflagration (see Figure 4-5), the high-pressure area of a real-cloud is larger compared with a hemispherical cloud, however, outside the cloud perimeter it decays more rapidly due to the narrower zone to which the pressure is restricted when propagating with the flame front (Geiger, 1982 as cited in Verfondern & Nishihara, 2005).

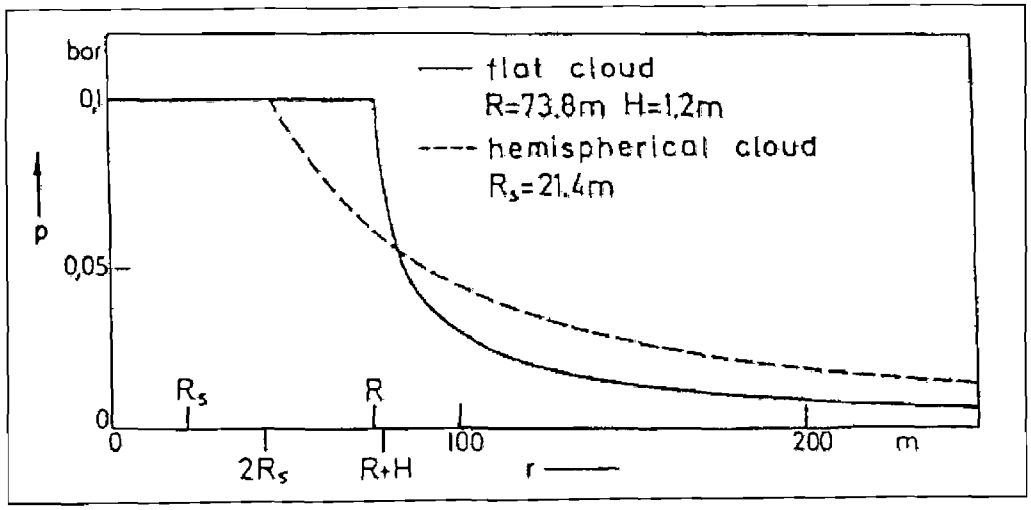

Figure 4-5: Deflagration pressure profile in a hemispherical and in a flat gas cloud (Verfondern & Nishihara, 2005)

The detonation front (Figure 4-6) propagates through the cloud without attenuation and most of its combustion energy generates a blast wave that rapidly decays

beyond the cloud perimeter. The high-pressure area, overpressure and positive-phase impulse of real-cloud detonations are much larger compared with that of hemispherical-cloud detonations (Verfondern & Nishihara, 2005).

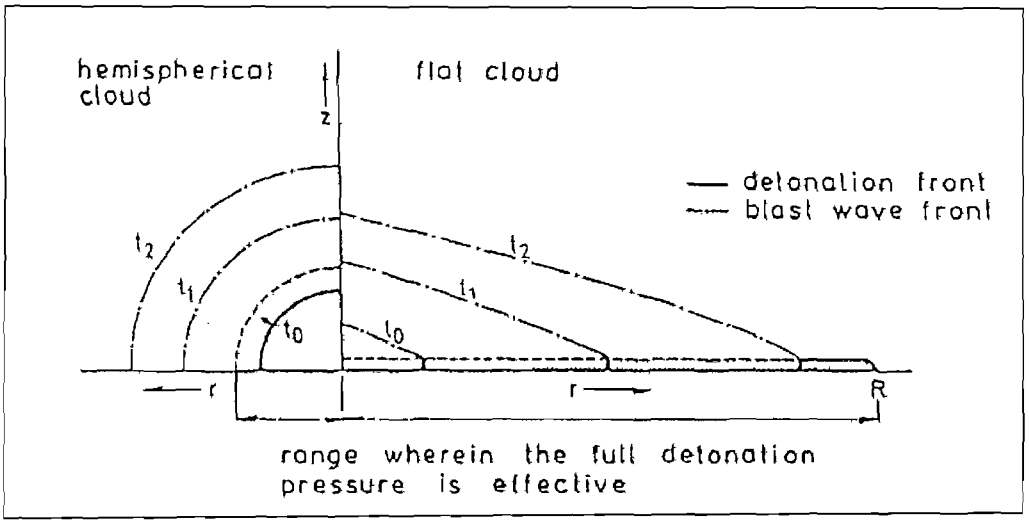

Figure 4-6: Detonation pressure profile in a hemispherical and in a flat gas cloud (Verfondern & Nishihara, 2005)

The explosive combustion of an unconfined hydrogen-air mixture releases only a fraction of its thermal energy content (0.1 to 10 %, usually < 1 %) and the magnitude of the shock wave depends on the mode of combustion (deflagration or detonation), with a peak deflagration-overpressure of approximately 10 kPa (Verfondern & Nishihara, 2005).

Lastly, the resultant dispersion of a hazardous substance may lead to an asphyxiation hazard somewhat similar to that of hydrogen, which is given in the following table (Table 4-2; NASA, 2005):

Table 4-2: Asphyxiation hazards of hydrogen (NASA, 2005)

15-19 percent by volume	Decreased ability to perform tasks; may induce early symptoms in persons with heart, lung, or circulatory problems
12-15 percent by volume	Deeper respiration, faster pulse, poor coordination
10-12 percent by volume	Giddiness, poor judgment, slightly blue lips
8-10 percent by volume	Nausea, vomiting, unconsciousness, ashen face, fainting, mental failure
6-8 percent by volume	Death in 8 min; 50 percent death and 50 percent recovery with treatment in 6 min, 100 percent recovery with treatment in 4 to 5 min
4 percent by volume	Coma in 40 s, convulsions, respiration ceases, death

4.3 IGNITION

Ignition of a flammable gas cloud is readily achieved for most of the flammable substances and mixtures present at a hydrogen production facility and even the electrostatic discharge by a person (10 mJ) is sufficient to ignite hydrogen-air or methane-air mixtures, which have minimum ignition energies of 0.29 mJ and 0.019 mJ respectively (Verfondern & Nishihara, 2005). According to US regulations, there shall be no sources of ignition in buildings or special rooms containing hydrogen systems, with the intention that ignition sources must be eliminated or safely isolated, and operations conducted as if unforeseen ignition sources could occur (NASA, 2005). While Table 4-3 lists the potential ignition sources for hydrogen systems, it is assumed that these sources are also applicable to methane systems since methane's minimum ignition energy is comparable to that of hydrogen.

Table 4-3: Potential Ignition Sources (Ordin, 1983 as given in NASA, 2005)

Thermal Ignition	Electrical Ignition
Personnel smoking	Electrical short circuits, sparks, and arcs
Open flames	Metal fracture
Shock waves from tank rupture	Static electricity (two-phase flow)
Fragments from bursting vessels	Static electricity (flow with solid particles)
Heating of high-velocity jets	Lightning
Welding	Generation of electrical charge by equipment operations
Explosive charges	
Friction and galling	
Resonance ignition (repeated shock waves in a flow system)	
Mechanical impact	
Tensile rupture	
Mechanical vibration	
Exhaust from thermal combustion engine	

The ignition of gaseous hydrogen-air mixtures usually results in ordinary deflagration, however, fast deflagrations, DDTs and detonations are possible in certain geometries under turbulent flow conditions (NASA, 2005).

4.4 COMBUSTION

In combustion processes, fuel and oxidizers violently react with another to form combustion products and release significant amounts of heat energy. These processes are categorized according to the state of the mixture before combustion (premixed or non-premixed) and whether the fluid flow is laminar or turbulent (Warnatz *et al.*, 2006). Turns (2000) defines a flame as being a self-sustaining propagation of a localized combustion zone at subsonic velocities. Moreover, a combustion wave travelling at subsonic velocities is termed a deflagration, whereas a detonation occurs when the combustion wave propagates at supersonic velocities. Since the fundamental propagation method of a detonation differs significantly from that of deflagrations, they are considered as distinct phenomena and investigated separately (Turns, 2000).

The essential features of a (laminar) flame is clearly illustrated in the following figure (Figure 4-7) and include the temperature profile, (volumetric) heat release rate and reactant concentration profiles (Warnatz *et al.*, 2006).

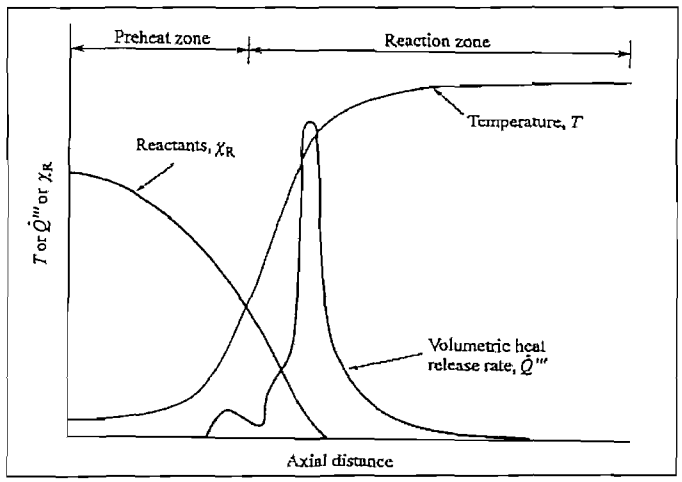

Figure 4-7: Essential features of a laminar flame (Friedman & Burke as illustrated in Warnatz *et al.*, 2006)

4.4.1 LAMINAR PREMIXED FLAME

In laminar premixed flames, the fuel and oxidizer are premixed before combustion and the flow of the fluid is laminar. Examples of laminar premixed flames are flat flames and Bunsen flames as are shown in the following figure (Figure 4-8, Wamatz *et al.*, 2006).

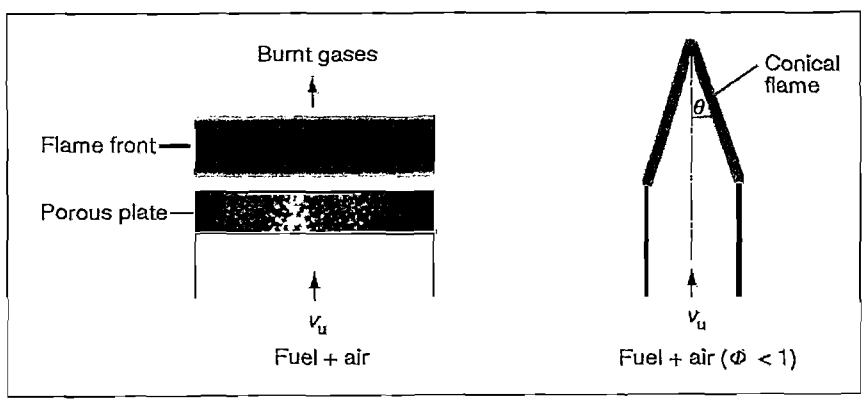

Figure 4-8: Laminar premixed flames with a flat flame and Bunsen flame illustrated on the left and right respectively (Warnatz *et al.*, 2006)

Premixed flames are at stoichiometric concentration when the fuel and oxidizer consumes each other completely during combustion to produce only water and CO_2,

whereas fuel-rich and fuel-lean combustions respectively have excess fuel or oxygen (oxidizer).

4.4.2 LAMINAR NON-PREMIXED FLAME

Laminar non-premixed flames are also known as laminar diffusion flames and mixing of the fuel and oxidizer occurs during combustion. The state of mixing allows differentiating between counter-flow and co-flow laminar diffusion flames (Figure 4-9), while laminar jet diffusion flames are also possible (Figure 4-10).

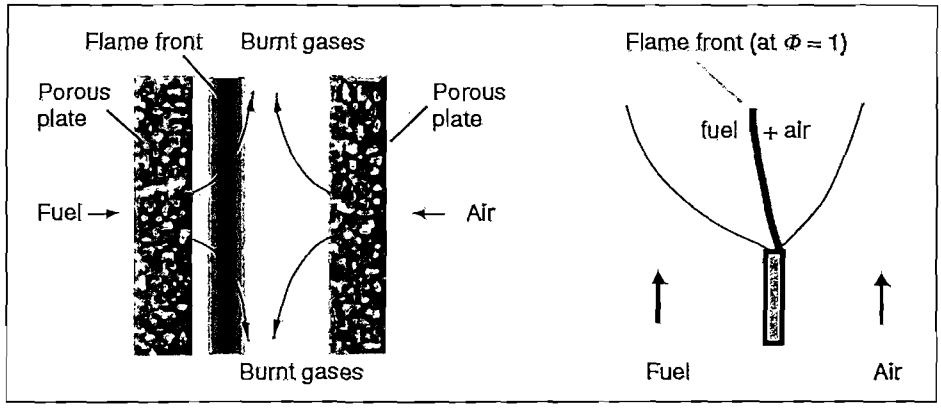

Figure 4-9: Schematic illustration of counter-flow and co-flow laminar diffusion flames (Warnatz *et al.*, 2006)

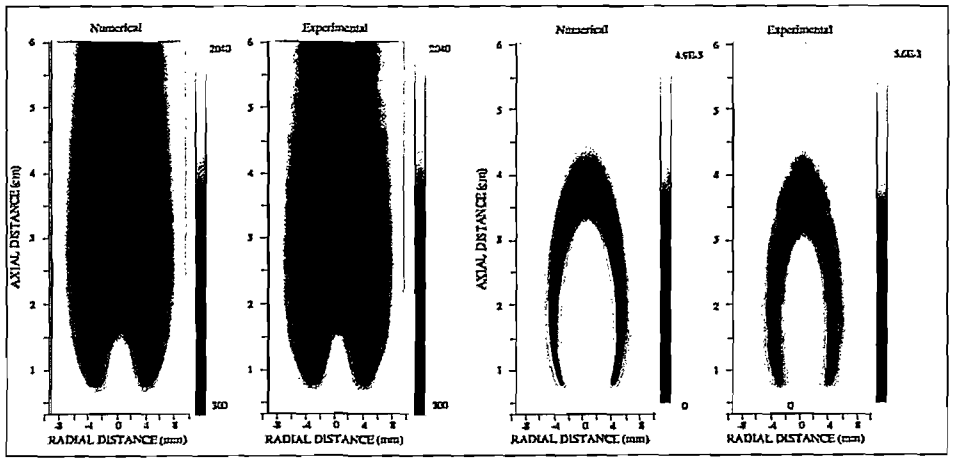

Figure 4-10: Laminar jet diffusion flames (Smooke et al, 1989 as illustrated in Warnatz *et al.*, 2006)

Figure 4-10 illustrates the calculated (numerical) and experimental fields of temperature on the left-hand side, as well as that of the OH-radical concentrations on the right-hand side for laminar jet diffusion flames (Warnatz *et al.*, 2006).

4.4.3 TURBULENT PREMIXED FLAME

In turbulent premixed flames, the fuel and oxidizer are premixed before combustion and the propagation of the flame is turbulent. Figure 4-11 is a schematic illustration of a "V-shaped" turbulent premixed flame, which is stabilized by the recirculation of hot gas behind a bluff body. While the outer edge of the "V" is smooth if the flow is laminar, the outer edge of a turbulent "V-shaped" flame is ragged (Warnatz *et al.*, 2006).

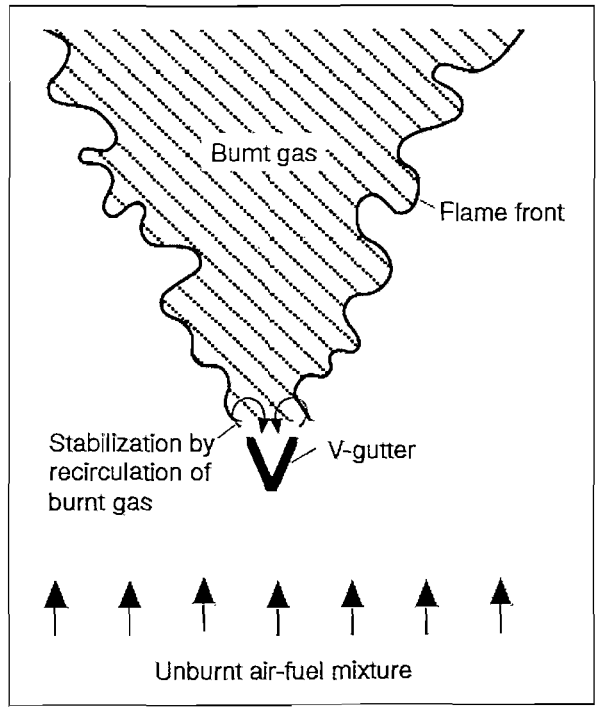

Figure 4-11: Schematic illustration of a "V-shaped" turbulent premixed flame stabilized by a bluff body (Warnatz *et al.*, 2006)

The departure of the turbulent premixed flame front from a plane to an increasingly three-dimensional structure is the subject of the Borghi diagram, which is shown in Figure 4-12 below. The Borghi diagram clearly illustrates the different flame fronts corresponding to the different premixed states and fluid flow rates (Borghi, 1984 as cited in Warnatz *et al.*, 2006).

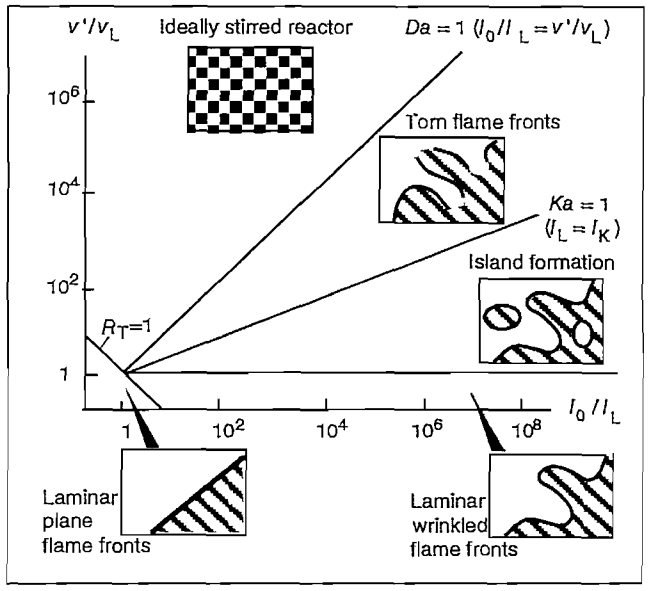

Figure 4-12: Borghi diagram (Borghi, 1984 as illustrated in Warnatz *et al.*, 2006)

4.4.4 TURBULENT NON-PREMIXED FLAME

A turbulent non-premixed (diffusion) flame is characterized by turbulent fluid flow of the fuel and oxidizer to "meet" at the origin of combustion. Figure 4-13 is a schematic illustration of a turbulent diffusion jet flame (Warnatz *et al.*, 2006).

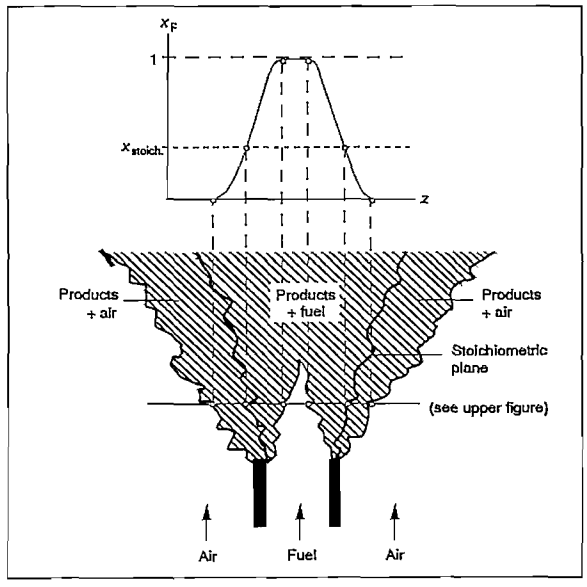

Figure 4-13: Schematic illustration of a turbulent diffusion jet flame (Warnatz *et al.*, 2006)

In practical applications of combustion such as jet engines, furnaces and rockets, turbulent non-premixed flames are safer than turbulent premixed flames since the fuel and oxidizer "meet" in the combustion chamber. The two-dimensional flame structure and temperature profile (contours) of a turbulent non-premixed methane-air jet flame is illustrated in the following figure (Figure 4-14; Nau *et al.*, 1996 as cited in Warnatz *et al.*, 2006)

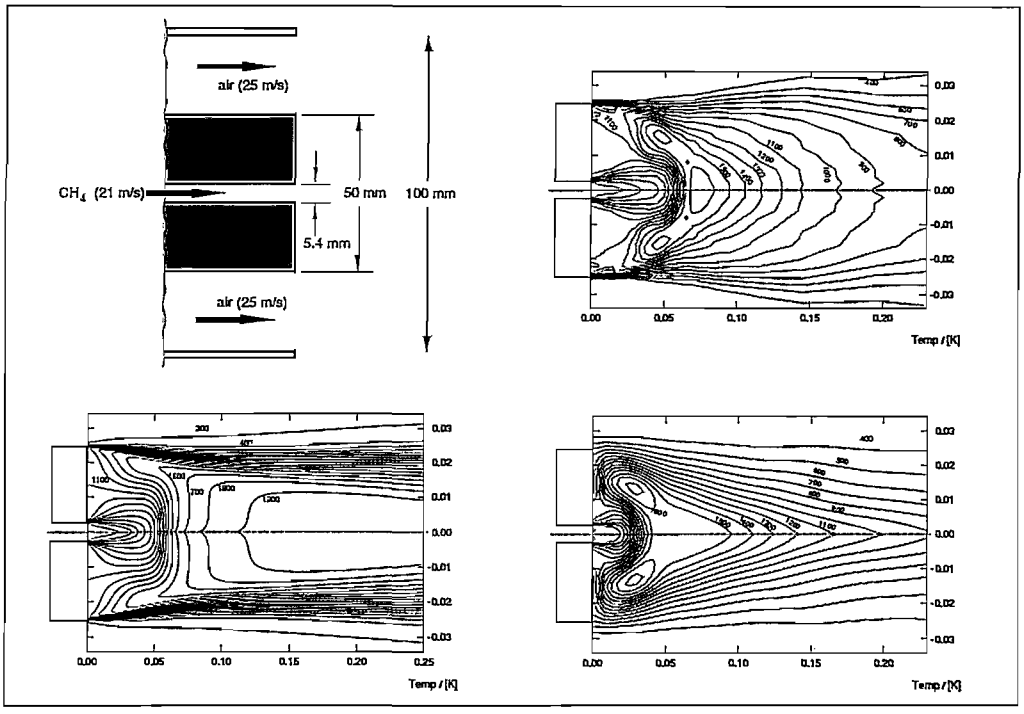

Figure 4-14: Turbulent non-premixed methane-air jet flame (Nau *et al.*, 1996 as illustrated in Warnatz *et al.*, 2006)

4.4.5 GENERAL TYPES OF COMBUSTION

4.4.5.1 FLASH FIRES & FIREBALLS

The continuous addition of heat to a stored liquid gas increases the internal pressure in the vessel until it bursts or ruptures. The liquid gas evaporates quickly and if ignited at an early stage, it results in a flash fire where the vapour cloud burns but does not explode. A diffusive flame develops without any significant flame acceleration and results in a spherical spreading of the flame front. The fire hazards associated with flash fires are primarily thermal radiation, direct flame impingement and oxygen depletion to humans in close vicinity of the fire (over-pressures are

negligible). The most frequent combustion encountered for unconfined clouds is the "fireball", which occurs from BLEVEs or jet releases when there is almost no mixing between the fuel and air and results in combustions of very rich mixtures. In fireballs, the diffusion flame propagates from the outside to the inside and coincides with the formation of considerable quantities of carbon (Verfondern & Nishihara, 2005).

4.4.5.2 UNCONFINED VAPOUR CLOUD EXPLOSION

The continuous release of a flammable gas into the atmosphere could result in the formation of a large, potentially flammable fuel/air cloud in which mixing with air has already taken place. If ignited belatedly, significant flame acceleration through the cloud is possible due to "inhomogeneities" in the cloud and disturbances of the flame symmetry. Flame acceleration is an effect enhanced by the presence of obstructions, which increases the turbulence of the fluid in close vicinity of the obstruction. The combustion of this cloud is an explosion if the release of energy occurs over a sufficiently short period, in a relatively small volume and generates a strong pressure wave. This event is an unconfined vapour cloud explosion (UVCE) and is the most serious hazardous event in the process industries (Verfondern & Nishihara, 2005).

The consequences of a vapour cloud explosion depend on several parameters such as fuel type, fuel concentration and size of the cloud, degree of initial turbulence, location and strength of the ignition source, degree of confinement, the presence of explosion vent areas and other explosion mitigation schemes. The magnitude of the generated pressure wave depends on the flame velocity and degree of congestion of the flammable cloud, and may be as high as 60 % of the total combustion energy of the flammable part of the vapour cloud. Flame speed and overpressure increase with degree of congestion due to the development of instabilities and self-confinement (associated with flammable clouds of large volume). The burning velocity is also an important parameter associated with flashbacks, which occur when the flame travels back to the source, especially when the velocity of the leaking gas is small. The distance that a flammable cloud can travel is unlikely to be very long in industrial or urban areas (Verfondern & Nishihara, 2005).

4.4.5.3 DEFLAGRATION

The most common mode of combustion of a flammable vapour cloud is deflagration of the flammable cloud and propagates by diffusion of the combustion products into

the unburnt gas. Deflagrations are associated with subsonic (< 1000 m/s) flame velocities and generate overpressures in the range of 0.1 to several 100 kPa. However, the cloud must be very large (at least 100 kg of methane at weak ignition) to generate a damaging pressure wave (Baker, 1983 as cited in Verfondern & Nishihara, 2005).

The flame front velocity determines the combustion process of a deflagration and is typical for each fuel. The propagation of the flame front (see Figure 4-15 for spherical flame front propagation) results in the generation of overpressure waves travelling at sonic speed into the unburnt mixture and into the surrounding environment. Therefore, the flame front velocity determines the amplitude of the pressure generated (up to a stagnation value; Verfondern & Nishihara, 2005).

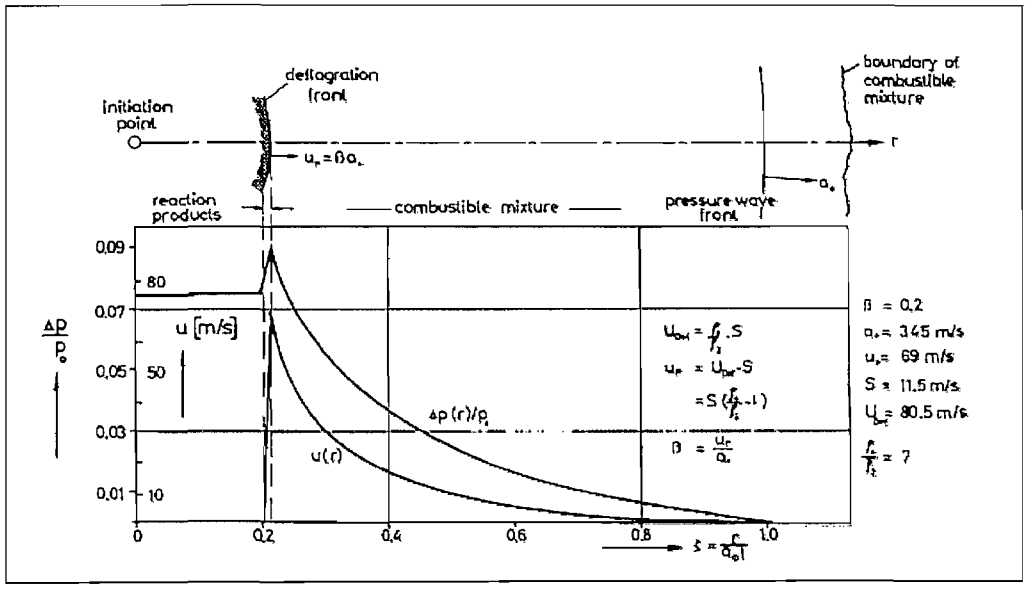

Figure 4-15: Overpressure and flow velocity distribution for a spherical deflagration wave (Verfondern & Nishihara, 2005)

4.4.5.4 DETONATION

A detonation is a combustion flame travelling at supersonic speeds (approximately 2000 m/s), where the flame front proceeds by shock wave compression of the unburnt gas and no expansion of the gas cloud occurs. Detonations generate significant peak overpressures (1.5 to 2 MPa) and according to the Chapman-Jouguet (CJ) theory, represents a discontinuity with infinite reaction rate. The

detonation velocity and the overpressure generated are determined by the equilibrium chemistry as a function of the gas mixture exclusively (Verfondern & Nishihara, 2005). Even though the processes inside the detonation front are extremely complex (multi-dimensional shock interactions, intensive turbulent reaction mediums), the CJ model for predicting the detonation velocity and overpressure is relatively accurate. To illustrate the specificity of CJ detonations, Figure 4-16 gives the Rankine-Hugenoit curve and shows that several other detonation modes are possible. Both weak and strong detonations have been observed experimentally, but most experimental conditions lead to CJ-detonations. The CJ detonation has the smallest propagation speed with hot gases travelling at the speed of sound, and a detonation wave with $\rho_0 v_0 = m$ (Warnatz *et al.*, 2006).

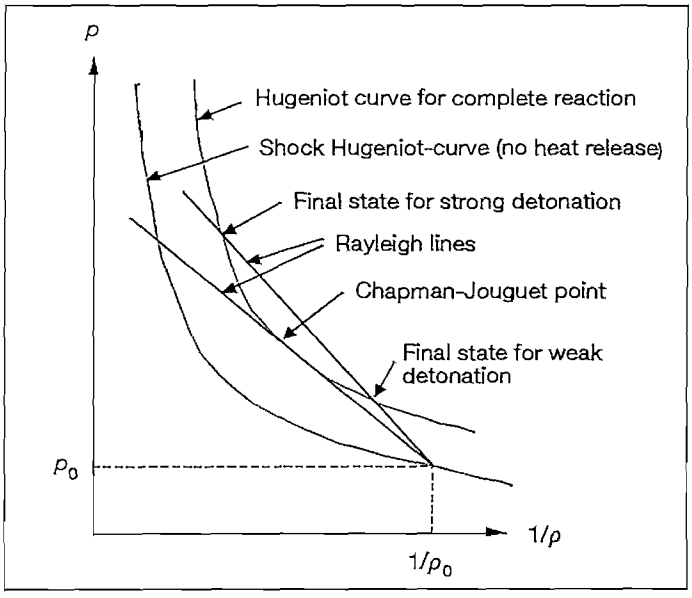

Figure 4-16: Rankine-Hugenoit curve (Warnatz *et al.*, 2006)

The transfer of a detonation wave into adjacent mixtures is possible for planar clouds, whereas in spherical clouds, fast deflagrations are more likely to occur. It is extremely unlikely that an unconfined hydrocarbon-air mixture will detonate; however, it is a requirement for any thorough safety and risk analysis (Verfondern & Nishihara, 2005).

Figures 4-17 and 4-18 illustrate the different characteristics of hydrogen deflagrations and detonations, specifically the flame acceleration, flame speed (as indicated by the time), geometry and heat radiation (as indicated by the IR photos).

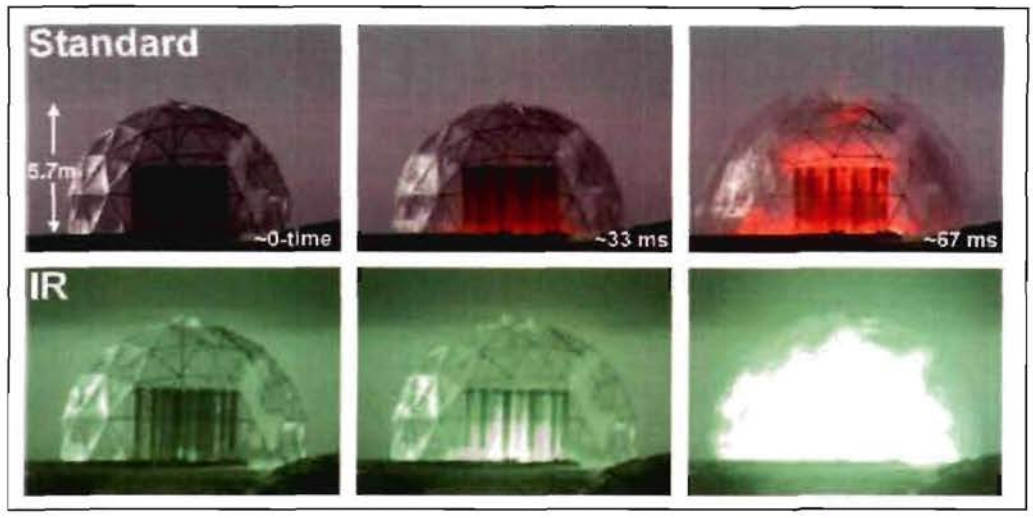

Figure 4-17: Obstacle experiment with 30% hydrogen mixture (Groethe *et al.*, 2007)

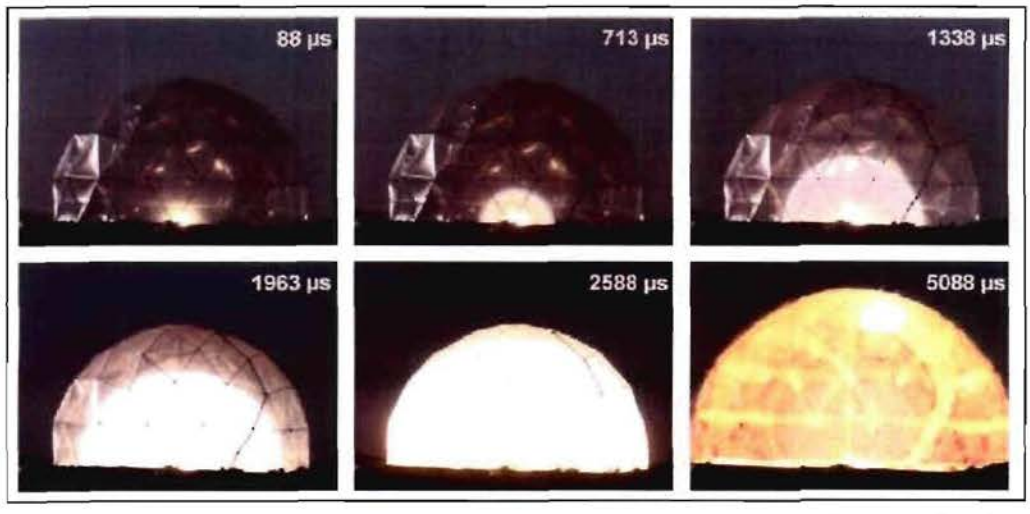

Figure 4-18: High-speed video frames from the detonation test (Groethe *et al.*, 2007)

An explosive can cause a detonation, but it is highly unlikely to occur at a typical industrial area due to the absence of an ignition source of sufficiently large (critical) energy (see Figure 4-19 below).

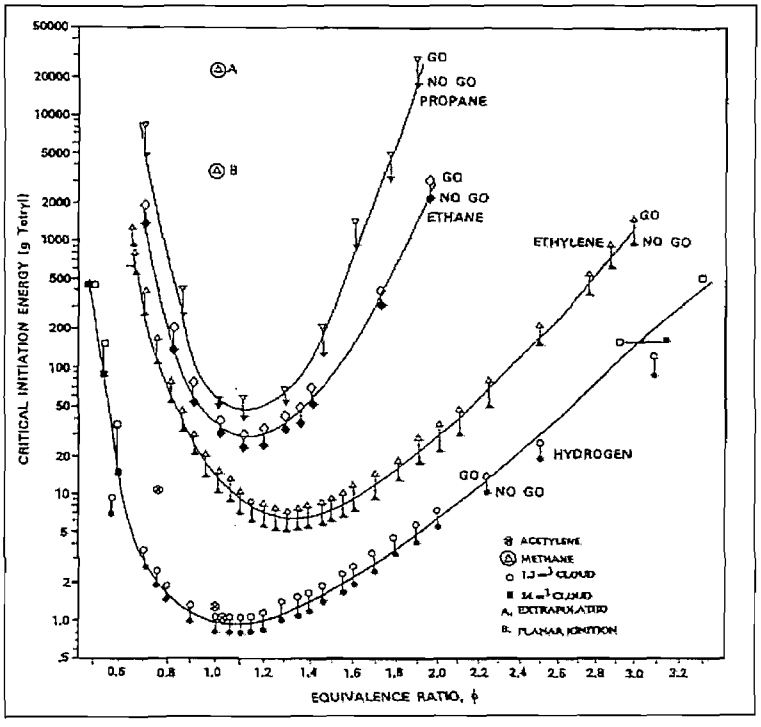

Figure 4-19: Critical initiation energy for selected fuel-air mixtures (Verfondern & Nishihara, 2005)

4.4.5.5 DEFLAGRATION-TO-DETONATION TRANSITION

The fundamental and quantifiable accelerating factors for the transition of a deflagration to a detonation are turbulence, turbulent burning velocity and regime of combustion. Turbulence plays a central role in all stages of DDT and the turbulent flow behaviour relies on the intensity and scale of turbulence. Several turbulent enhancing mechanisms exist that may influence the combustion process in a vapour cloud in an industrial area and include atmospheric turbulence, heat radiation transport by dust particles, local explosions behind the flame front, degree of obstruction and congestion, jet ignition (very important), Raleigh-Taylor instabilities and buoyancy acceleration (Verfondern & Nishihara, 2005).

The time scale for acceleration must be small compared to the hydrodynamic processes that relieve the increase in pressure. Pre-compression of the unburnt gas by the front pressure wave occurs at flame speeds greater than 300 m/s and enhances the acceleration process. The flame front velocity reaches a maximum when the counteracting effects of an enhanced mixture process and the temperature

decrease due to the mixing are in equilibrium. High flame speeds and pressures in tubes, pipes, confined channels and areas covered by a roof are reached within less than four diameters (Verfondern & Nishihara, 2005).

Many mechanisms supporting a detonation are not present in an unconfined gas cloud; however, the turbulent burning velocity mechanism is present and is given by the following relation (Koch, 1975 as given in Verfondern & Nishihara, 2005).

$$u_{turb} = \varepsilon f_T u_{lam}$$ **Equation 4-10**

With:

$$\varepsilon = \frac{T_2}{T_1}$$ **Equation 4-11**

Where:

u_{turb}	Turbulent burning velocity [m/s]
u_{lam}	Laminar burning velocity [m/s]
ε	Expansion factor [-]
f_T	Empirical turbulence factor in the order of 2 to 7[-]
T_1	Temperature of the reactants [K]
T_2	Temperature of the combustion products [K]

An estimation of the flame speed in hydrocarbon/air mixtures is in the range of 3 to 44.8 m/s and at very high turbulence levels quenching occur that decrease the turbulent combustion velocity (Verfondern & Nishihara, 2005).

The different regimes of premixed combustion during the DDT is shown in the so-called Schlieren pictures (Figure 4-20) and demonstrates the intricate interplay between hydrodynamic flow and chemistry. The regimes are laminar deflagration, turbulent deflagration and quasi-detonation and depend on the fuel content in the fuel/air mixture. Thus, by varying the fuel content the combustion mode changes. Figure 4-20 represents the regimes of premixed combustion for a hydrogen/air mixture with dark areas indicating high gradients in density (Verfondern & Nishihara, 2005).

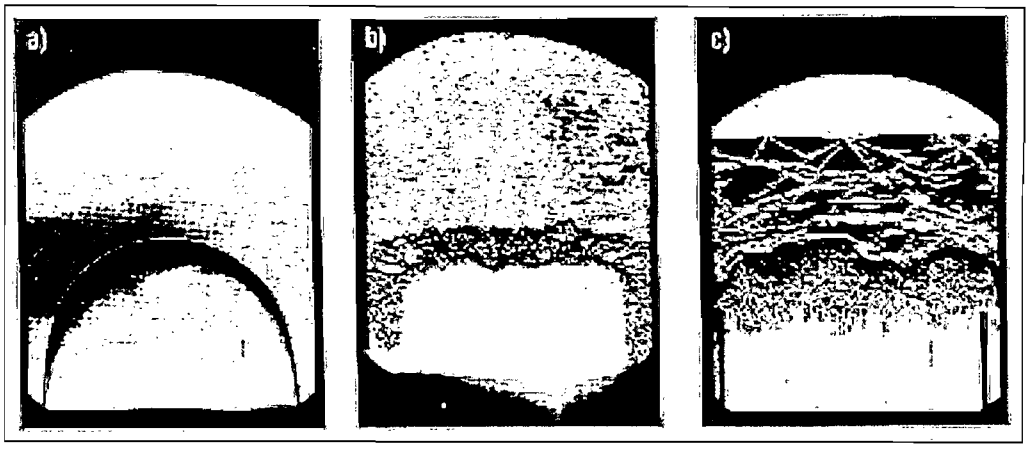

Figure 4-20: Schlieren pictures of a) a laminar deflagration, b) a turbulent deflagration, and c) a quasi-detonation (Verfondern & Nishihara, 2005).

Picture a) depicts a laminar deflagration occurring at lean H_2 concentrations of 9 to 10 vol%, has laminar burning velocities of less than 200 m/s, and a smooth thin flame front separating the unburnt and burnt gases. Picture b) represents a turbulent deflagration and occurs at H_2 concentrations of ± 12 % with fast turbulent flames characterized by pockets of unburnt and burnt gas surrounding each other, thereby increasing the flame front and the burning rate. Picture c) illustrates a quasi-detonation that occurs at high H_2 concentrations (> 15 %) and is associated with very high burning velocities (> 2000 m/s) resulting in the generation of pressure waves that increase the temperature the unburnt gas beyond its auto-ignition temperature in microseconds. A velocity-distance diagram (Figure 4-21) of the three combustion regimes shows that (Verfondern & Nishihara, 2005):

1. Lean H_2 concentrations (9 to 10 %) result in subsonic flames (< 200 m/s) with almost no flame acceleration.
2. Increased H_2 concentrations (± 12 %) is associated with fast turbulent combustion, has an initial acceleration phase and result in flame speeds up to the sound velocity.
3. High H_2 concentrations (± 15 %) reach the level of quasi-detonation after an initial acceleration phase with very high flame velocities.
4. Higher H_2 concentrations (> 20 %) develop into a stable detonation with a velocity of approximately the theoretical CJ speed (> 2000 m/s).

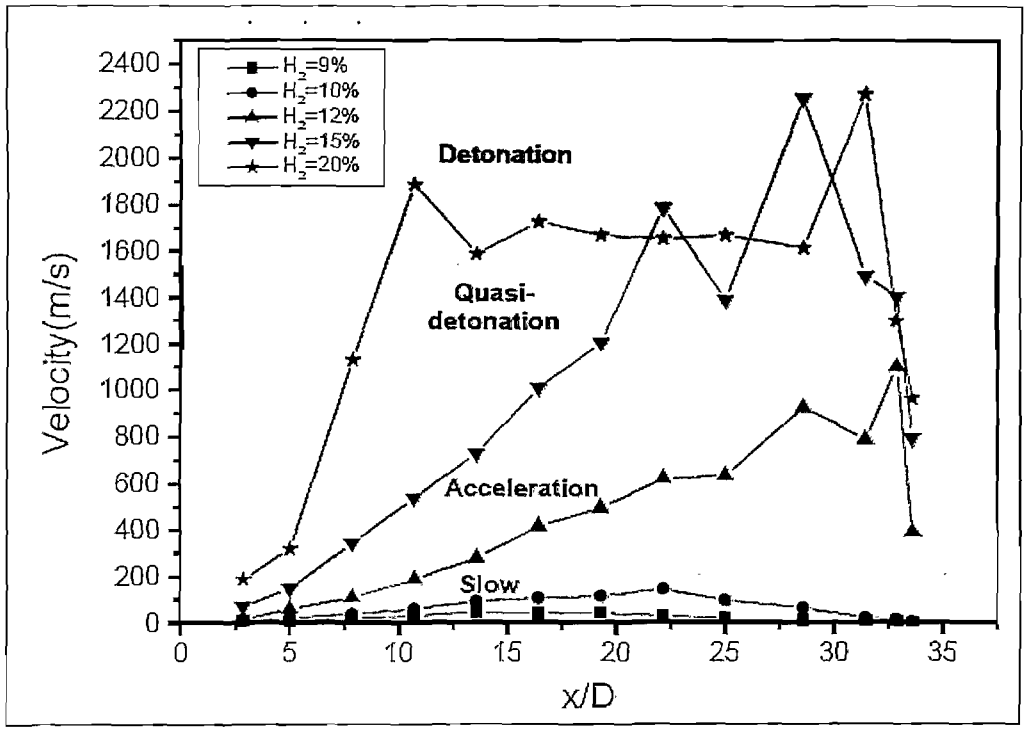

Figure 4-21: Velocity-distance diagram of FZK tube experiments with various H_2/air mixtures (Verfondern & Nishihara, 2005).

4.5 BLAST WAVES

A significant portion of the explosion energy is associated with developing a uniformly distributed blast wave and is an effect most pronounced at ground level, hemispherical explosions (two times the respective yield of a spherical explosion; Verfondern & Nishihara, 2005).

In a deflagration, the volume expansion caused by the combustion process displaces the unburnt gas, whereas a detonation generates a compression wave (spike) followed by a pressure decrease to below atmospheric conditions (molecular collapse). Over long distances, the pressure wave for both deflagration and detonation decays with 1/r. The following figure (Figure 4-22) shows the pressure functions for both of the combustion modes (Verfondern & Nishihara, 2005)

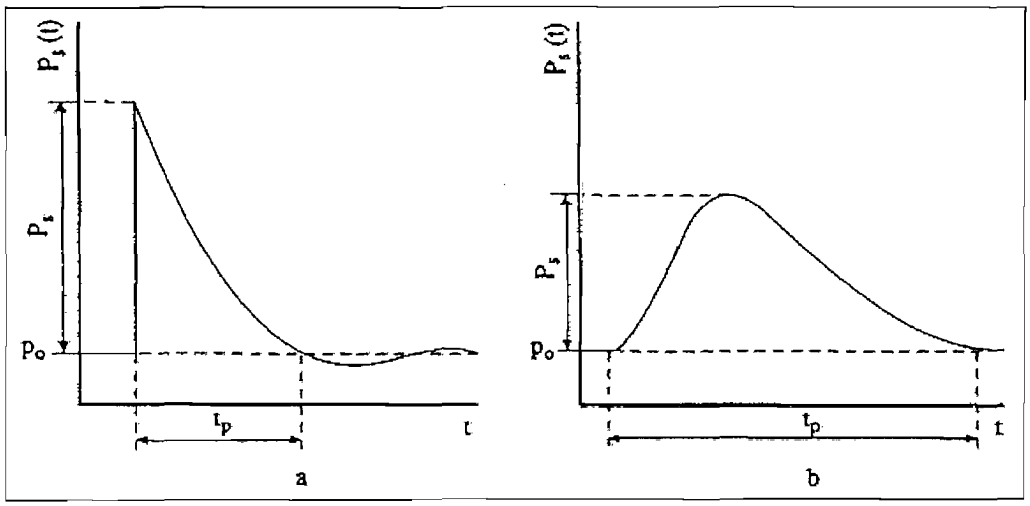

Figure 4-22: Characteristic shape of pressure-time function for a detonation shock wave on the Left and a deflagration pressure wave on the Right (Verfondern & Nishihara, 2005)

Deflagration and detonation differ in peak overpressure, duration of the pressure impulse, steepness of the wave front, and in the decrease of overpressure with propagation distance (Verfondern & Nishihara, 2005).

A very simple method to model blast effects is the TNT Equivalent method, but the model is inaccurate since it overestimates "near field" and underestimates "far-field" effects. A more suitable model is the Multi-Energy method developed by TNO, which suggests that a damaging explosion exclusively occurs when flame acceleration takes place within a plant structure. Special "blast charts" (Figure 4-23) show the relationship between a "scaled blast overpressure" (the ratio of blast overpressure over ambient overpressure) and a "scaled distance" (Mercx, 2000 as cited in Verfondern & Nishihara, 2005).

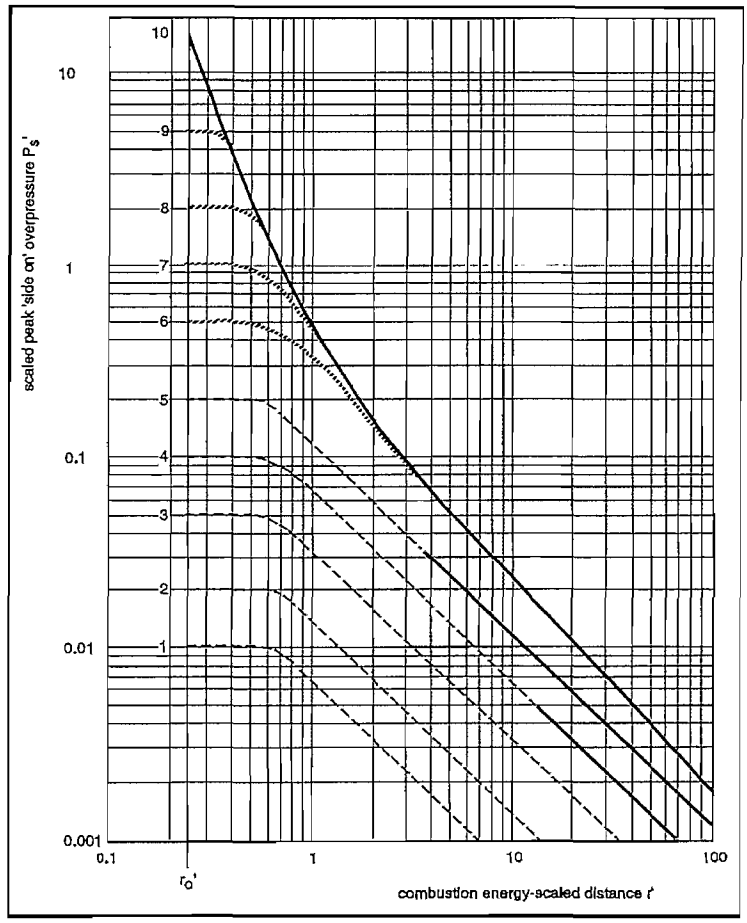

Figure 4-23: TNO for blast overpressure according to the Multi-Energy method (Verfondern & Nishihara, 2005)

The physiological hazard of blast overpressures are summarized in the following table (Table 4-4; NASA, 2005):

Table 4-4: Physiological hazard of overpressures (NASA, 2005)

Overpressure	Physiological Hazard
3 psi	1 % eardrum rupture
16 psi	20 % eardrum rupture
10 psi for 50 ms 20 – 30 psi for 3ms	Threshold of lung rupture
27 psi for 50 ms 60 – 70 psi for 3 ms	1 % mortality

Many pressure criteria have been defined related to various structures and specific components, however, they varying over a large uncertainty range and a rough classification thereof is given in Table 4-5 (Verfondern & Nishihara, 2005).

Table 4-5: Damage classification (Verfondern & Nishihara, 2005)

Zone	Damage Level	Overpressure of incident blast wave
A	Total destruction	> 83 kPa
B	Heavy damage	> 35 kPa
C	Moderate damage	> 17 kPa
D	Minor damage	> 3.5 kPa

For industrial installations, the limits in Table 4-6 are to be met for the control building (TNO, 1992 as cited in Verfondern & Nishihara, 2005):

Table 4-6: Control building specifications regarding overpressure (TNO, 1992 as given in Verfondern & Nishihara, 2005)

Type	Construction object	Overpressure	Duration
Pressure wave,	Walls	30 kPa	100 ms
	Roof	20 kPa	
Shock wave	Walls	300 kPa	15 ms
	Roof	200 kPa	

4.6 HEAT RADIATION

Approximately 75 % of the heat transfer from a fire is by convection to the surrounding atmosphere from the hot combustion products, with the remaining 25 % primarily associated with heat radiation. The fraction of combustion energy released as thermal radiation is 17 to 25 % for a hydrogen-air combustion and 23 to 33 % for a methane-air combustion. The simplest method for determining the thermal radiation energy released is the "Point Source Method" given by (Verfondern & Nishihara, 2005):

$$D = 0,28\left(\frac{FW_bC_v}{K_r}\right)^{1/2} \qquad \textbf{Equation 4-12}$$

With:

C_v Fuel caloric value [kJ/kg]

D Distance from the flame centre point [m]

F Fraction of combustion heat radiated [-]

K_r Allowable radiation level [-]

W_b Burning rate [kg/s]

The limitation of this method lies in its assumption that all radiation comes from the flame centre point and is therefore not extremely accurate. The following table (Table 4-7) shows the critical heat radiation data associated with humans and some goods (Verfondern & Nishihara, 2005).

Table 4-7: Critical heat radiation for humans and goods (Böke, 1995 as given in Verfondern & Nishihara, 2005)

Object	Time Period [s]	Heat Radiation [kW/m^2]
Max radiation strength for skin	any	< 1.7
Dolor tolerable	< 20	4
	< 13	5
1st Grade Burn	> 8	6.4
	> 3	10.4
2nd Grade Burn	> 10	10.5
	> 16	16
Blister formation	10 to 12	10.5
Lethal	> 40	10
Sensitive buildings	-	1 to 2
Public roads	-	4.5
Factory building	-	8 to 12.6
Not-cooled storage tank	-	10
Instantaneous ignition of wood	-	16 to 25
Cooled storage tank	-	37.8
Auto-ignition of wood fibre sheets	-	52

4.7 HYDROGEN EMBRITTLEMENT

Hydrogen affects the mechanical behaviour of materials by changing their physical properties such that they become brittle, thus the term hydrogen embrittlement. During hydrogen embrittlement, hydrogen atoms are dissolved into the metal grid of the material and accumulate in the disturbed lattice regions, thereby changing their mechanical properties (IAEA, 1999). In order to describe this effect, a quick overview of ductile and brittle behaviour of metals is required and is graphically represented in the following figure (Figure 4-24). This figure shows that all materials deform under load, but that ductile materials are able to deform substantially more than brittle materials before rupturing, as well as that the ultimate tensile strength of ductile material is generally above the threshold strength of brittle material. Considering ductile materials, elastic materials are able to return to their original state after deformation in shape and volume while the stress is below the material's yield strength. Above the yield strength of the material, permanent deformation in shape occurs while the volume remains constant. A further increase in stress above the ultimate tensile strength of the material results in a decrease in stress leading up to

rupturing. Thus, in ductile materials below their ultimate tensile strength, the molecular bonds gradually break and re-form while bending and reshaping without breaking, whereas in brittle materials all molecular bonds break almost immediately at a certain stress (ultimate tensile stress or threshold stress). Resultantly, ductile materials have approximately the same tension and compression strength, while brittle materials have much higher compression than tension strength (BRHS, 2007).

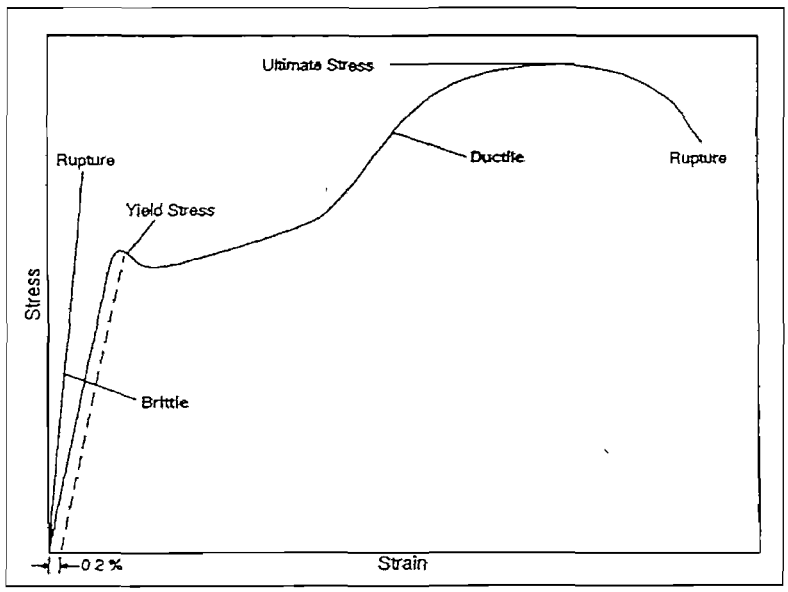

Figure 4-24: Ductile and brittle behaviour of metals (Verfondern, 1999 as illustrated in BRHS, 2007 and IAEA, 1999)

Hydrogen embrittlement is a long-term effect that occurs from continued use of a hydrogen system during production, transport, storage and use. According to a report by NASA (2005):

> *"hydrogen embrittlement involves a large number of variables such as the temperature and pressure of the environment; the purity, concentration, and exposure time of the hydrogen; and the stress state, physical and mechanical properties, microstructure, surface conditions, and nature of the crack front of the material."*

4.7.1 PHENOMENA

It is important to note that the phenomena of hydrogen embrittlement depend on whether atomic or molecular hydrogen is present to embrittle the material. Molecular hydrogen, such as is usually produced in the nuclear-assisted hydrogen production technologies, is extremely stable and should not pose a significant hydrogen embrittlement hazard. However, atomic hydrogen has a high tendency to diffuse into metals and cause hydrogen embrittlement that seriously reduces the ductility and load-bearing capacity of the material, and causes cracking and catastrophic brittle failures at stresses below the yield stress of susceptible materials (BRHS, 2007). In this regard, it is universally accepted that hydrogen in its atomic form and not as a molecule can cause embrittlement when present in a metal or alloy. This is due to the dissolved hydrogen atoms concentrating in defects of the crystal structure of the material, thereby impeding the movement of dislocations (breaking and re-forming of bonds) and decreasing the material's ductility, which make it brittle. However, at elevated temperatures (above 473 K) the presence of molecular or atomic hydrogen concentrations at grain boundaries can result in the formation of hybrids when hydrogen reacts with the metal to cause hydrogen embrittlement (possibly the decarburization of the metal if hydrogen reacts with the carbon constituent of the metal).

According to a report by BRHS (2007), atomic hydrogen enters the metal via several mechanisms, including the following (as quoted from the source):

- *"via dissolution during welding, while the metal melts locally dissolving hydrogen from water or other contaminants;*
- *via electrochemical processes, such as surface treating or aqueous corrosion, where molecular hydrogen dissociates into atoms that diffuse into the metal;*
- *via chemisorptions, resulting from van der Waals forces between a metal surface and hydrogen molecules also resulting in the dissociation of the hydrogen molecules into atoms."*

Depending on the state of hydrogen (atomic or molecular), the concentration of hydrogen exposed to the metal and the temperature of the metal, hydrogen embrittlement can be categorized into three categories.

4.7.2 CATEGORIES

According to the IAEA (1999), research on the effect of hydrogen embrittlement has led to the definition of three different categories, which as quoted from this source, are:

a) *"**Hydrogen Reaction Embrittlement:** Hydrogen reaction embrittlement is a phenomenon in which the hydrogen chemically reacts with a constituent of the metal to form a new micro-structural element or phase such as a hydride or gas bubbles ("blistering"), e.g., methane gas if combined with carbon, or steam if combined with oxygen. These reactions usually occur at higher temperatures. They result in the formation of blisters or expansions from which cracks may start to weaken the metal.*

b) ***Internal Hydrogen Embrittlement:** Internal hydrogen embrittlement means that hydrogen is introduced into the metal during its processing, e.g., chemical reactions with water to form metal oxide and liberate hydrogen. It is a phenomenon that may lead to the structural failure of material that never has been exposed to hydrogen before. Internal cracks are initiated showing a discontinuous growth. Not more than 0.1 -10 ppm hydrogen in the average are involved. The effect is observed in the temperature range between -100 and +100 °C and is most severe near room temperature.*

c) ***Environmental Hydrogen Embrittlement:** Environmental hydrogen embrittlement means that the material was subjected to a hydrogen atmosphere, e.g., storage tanks. Absorbed and/or adsorbed hydrogen modifies the mechanical response of the material without necessarily forming a second phase. The effect occurs when the amount of hydrogen that is present, is more than the amount that is dissolved in the metal. The effect strongly depends on the stress imposed on the metal. It also maximizes at around room temperature."*

The following table (Table 4-8) summarizes the typical characteristics of the different hydrogen embrittlement types as given in the report by NASA (2005).

Table 4-8: Typical characteristics of hydrogen embrittlement types (NASA, 2005)

Characteristic	Environmental Hydrogen Embrittlement	Internal Hydrogen Embrittlement	Hydrogen Reaction Embrittlement
Usual source of hydrogen	Gaseous hydrogen	Processing, electrolysis, corrosion	Gaseous or atomic hydrogen from any source.
Typical conditions	10^{-6} to 10^{-8} Pa H_2 gas pressure. Most severe near room temperature. Observed from -100 to 700 °C. Gas purity and strain rate important.	0.1 to 10 ppm average H_2 content. Most severe near room temperature. Observed from -100 to 100 °C. Strain rate is important.	Heat treatment or service in H_2, especially at elevated temperatures.
Test methods for embrittlement	Notched tensile; unnotched tensile, creep rupture; fatigue (low, high cycle); fracture toughness; disk pressure test.	Notched tensile delayed failure; slow strain rate tensile; bend tests; C-rings; torqued bolts.	Visual or metallographic observation.
Location of crack initiation	On surface or internal. [b]	Internal crack initiation; incubation (reversible); slow discontinuous growth; and fast fracture.	Usually internal initiation from bubbles or flakes.
Rate-controlling embrittlement step	Adsorption is transfer step; absorption or lattice diffusion [b] is embrittling step.	Lattice diffusion to internal stress risers.	Chemical reaction to form hydrides or gas bubbles.

[a] Gray H. R., "Testing for Hydrogen Environment Embrittlement: Experimental Variables," *Hydrogen Embrittlement Testing*, American Society for Testing and Materials, Special Technical Publication, ASTM STP-543, Philadelphia, PA (1974), pp. 133-151.
[b] Unresolved

4.7.3 MECHANISMS

According to a report by BRHS (2007), several mechanisms have been proposed that might be able to explain, at least partially, the degradation of metal by hydrogen embrittlement. These mechanisms may act simultaneously or individually and, as quoted from this source, are:

- *"The formation of hydrides can lead to new hydrogen-related phases that may be brittle and may have a lower density than the pure metal leading to internal stress.*
- *The hydrogen distribution in a metal under stress is highly non-uniform which can lead to locally increased hydrogen-enhanced plasticity causing local microscopic deformation and eventually a failure.*
- *The lattice de-cohesion effect is presumed to cause embrittlement by a decrease in the atomic bonding strength in the presence of hydrogen. A fracture occurs when the stress exceeds the cohesive stress.*

- *Molecular hydrogen precipitation forming high pressures and compound formation are other mechanisms identified."*

Therefore, the metal and its metallurgical history influence the material's susceptibility to hydrogen embrittlement due to affecting the migration behaviour of hydrogen within the metal. Additionally, hydrogen embrittlement is significantly dependent on high, localized hydrogen concentrations as a result of stress-enhanced diffusion rates to lattice defects and reaction sites to initiate cracks. These cracks grow above a critical hydrogen concentration but end when the hydrogen concentration is low or when the stress factor has decreased sufficiently (BRHS, 2007).

4.8 CONCLUDING REMARKS

In this chapter, the accident phenomena associated with the evolution of a gaseous cloud, ignition and combustion of a flammable gas cloud, the consequences of combustion, and hydrogen embrittlement were examined. From the discussions of the hazardous substances (Chapter 3) and evolution of gaseous clouds, it is clear that heavier-than-air substances will significantly affect the safety of the nuclear plant. However, flammable hydrogen-air gas clouds will not have a substantial affect on the safety of the nuclear facility considering the most probable outcomes arising from the combustion of a free, flammable hydrogen-air gas cloud. During this event, the energy of combustion is in the range of 0.1 – 10 % of the thermal energy content of the gas cloud (usually less than 1%), of which only a fraction (17 – 25 %) is radiated to the surroundings and will generate a pressure wave in the range of 10 kPa. These consequences of combustion will not be significant barriers to the safety and implementation of a combined nuclear/chemical complex, however, they may well be of regulatory concern. Considering hydrogen embrittlement, due to the hydrogen produced at the production facilities being of molecular state, which is extremely stable, hydrogen embrittlement will not be a major issue to address. However, if the long operating lifetimes and the severe operating conditions of the facilities are taken into account, hydrogen embrittlement should be considered in the designs, material selections and probabilistic safety assessments. Since the hazardous substances and their propagation methods are known, they can be evaluated with regard to their attendant risk to the combined nuclear/chemical complex, which subsequently forms the next topic of discussion.